

[Chem. Pharm. Bull.]
34(8)3087—3096(1986)

Vibrational Spectra, Normal Coordinates and Infrared Intensities of Aspirin Crystal

YESOOK KIM and KATSUNOSUKE MACHIDA*

*Faculty of Pharmaceutical Sciences, Kyoto University, Yoshida
Shimoadachi-cho, Sakyo-ku, Kyoto 606, Japan*

(Received February 20, 1986)

A model potential consisting of the exp-6 type dispersion and exchange repulsion terms, the Lippincott type hydrogen bond stretching terms and the electrostatic interaction terms between fixed atomic charges was applied for elucidation of the vibrational spectra of aspirin crystal. The frequencies of the optically active inter- and intramolecular normal modes were calculated. The proposed potential reproduced the factor group splittings between the infrared (IR) and Raman frequencies and the lattice vibrational frequencies equally well. The IR spectra of aspirin and its -COOD analogue were simulated by using the calculated normal frequencies and a simple charge flux model.

Keywords—aspirin; infrared spectrum; Raman spectrum; normal frequency; lattice vibration; intermolecular potential; infrared intensity; atomic charge

Introduction

In a previous study we simulated the equilibrium atomic coordinates and the elastic constants of aspirin crystal ($C_6H_4(OCOCH_3)COOH$) successfully on the basis of a set of model potential functions representing the intra- and intermolecular forces.¹⁾ Using the same potential parameters, we calculated the specific surface energies of the main crystalline surfaces *in vacuo* and in contact with continuous media with various dielectric constants. The relative rates of diminution of the surface areas on dissolution of the aspirin single crystal in water were found to be correlated closely with the extent to which the Coulomb interaction contributes to the surface energy.²⁾ Consequently, we attempted to check the consistency between the potential parameters used in these studies and the vibrational spectra of aspirin crystal. The calculated optically active normal frequencies were in good agreement with those assigned in the infrared (IR) and Raman spectra of aspirin and its -COOD analogue. Based on the calculated normal modes of the isolated molecular model, the IR spectra were simulated with a simple model of the atomic charges and their fluxes along the internal coordinates. The quadratic intramolecular force constants were taken from those of benzoic acid (C_6H_5COOH) and phenyl acetate ($C_6H_5OCOCH_3$), from our two previous studies,^{3,4)} which also furnished useful information for carrying out the IR intensity calculations on aspirin in the present work.

Experimental

Single crystals of JP grade aspirin were grown from saturated ethanolic solutions at room temperature as monoclinic plates. The aspirin-COOD was prepared from its heavy water solution.

The IR spectra of KBr tablets between 400 and 4000 cm^{-1} were recorded on a JASCO-A2 grating spectrophotometer, and those between 500 and 200 cm^{-1} on a JASCO DS403G spectrophotometer. A large single crystal ($6.9 \times 7.4 \times 1.3 \text{ mm}^3$) was sliced along the cleavage plane, face (100),²⁾ to form a layer of uniaxially oriented fibrous crystallites. The polarized IR spectra of the a_u and the b_u modes were recorded for this sample, by using

incident radiations with the electric vector parallel and perpendicular, respectively, to the b crystal axis. The Raman spectra were observed on a JEOL S-1 laser Raman spectrophotometer equipped with a Coherent Radiation model 52G Ar⁺ laser. The 488.0 nm line was used as the exciting source with an output power of about 110 mW at the sample position. The sample of aspirin-COOD was sealed in a 1 mm capillary tube, while the undeuterated aspirin was subjected to measurement as a single crystal.

Theoretical

Normal Coordinate Analysis

The optically active normal frequencies of aspirin and aspirin-O- d crystals were calculated by using the dynamical matrices written in terms of the normal coordinates of the isolated molecular model.⁵⁾ We assumed the intermolecular potential to consist of the same three types of terms as previously used for the calculation of the specific surface energy of aspirin crystal.²⁾ They are the exp-6 type non-bonded potential (V_1), the Lippincott type hydrogen bond stretching potential (V_2)⁶⁾ and the Coulomb potential including the complementary error function as a convergence factor (V_3).⁷⁾ This potential was supplemented with a coupling term between the equivalent C=O stretching coordinates of each ring dimer.³⁾ The summation limits for V_1 and V_3 are the same as those used in our previous report for the crystal structure of aspirin.¹⁾ The atomic charges for V_3 were partly modified to reproduce the IR intensities as discussed later.

The lattice constants and the atomic coordinates were taken from our crystal data.¹⁾ The internal coordinates used in the calculation are shown in Fig. 1, and the internal symmetry

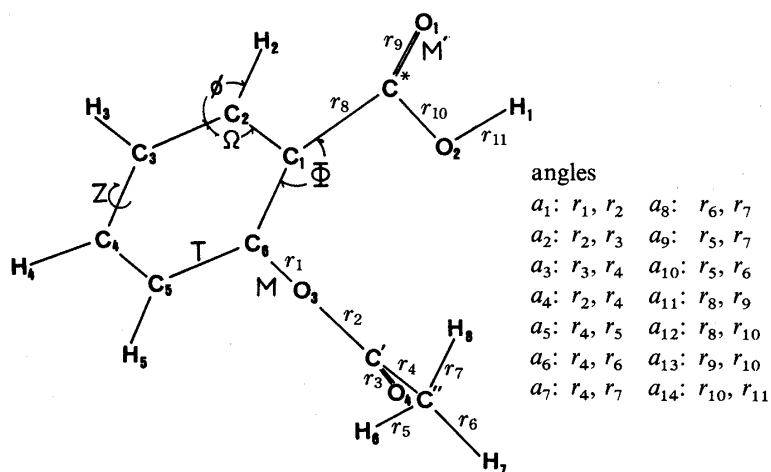


Fig. 1. The Structure and Internal Coordinates Used in the Calculation

TABLE I. Internal Symmetry Coordinates for the Stretching and Bending Modes of the Substituents

$S_1 = \Delta r_1$	$S_{12} = \sqrt{6}^{-1}(2\Delta a_8 - \Delta a_9 - \Delta a_{10})$
$S_2 = \Delta r_2$	$S_{13} = \sqrt{6}^{-1}(2\Delta a_5 - \Delta a_6 - \Delta a_7)$
$S_3 = \Delta r_3$	$S_{14} = \sqrt{2}^{-1}(\Delta a_{10} - \Delta a_9)$
$S_4 = \Delta r_4$	$S_{15} = \sqrt{2}^{-1}(\Delta a_6 - \Delta a_7)$
$S_5 = \sqrt{3}^{-1}(\Delta r_5 + \Delta r_6 + \Delta r_7)$	$S_{16} = \Delta r_8$
$S_6 = \sqrt{3}^{-1}(2\Delta r_5 - \Delta r_6 - \Delta r_7)$	$S_{17} = \Delta r_9$
$S_7 = \sqrt{2}^{-1}(\Delta r_6 - \Delta r_7)$	$S_{18} = \Delta r_{10}$
$S_8 = \Delta a_1$	$S_{19} = \Delta r_{11}$
$S_9 = \sqrt{6}^{-1}(2\Delta a_4 - \Delta a_2 - \Delta a_3)$	$S_{20} = \sqrt{6}^{-1}(2\Delta a_{13} - \Delta a_{12} - \Delta a_{11})$
$S_{10} = \sqrt{2}^{-1}(\Delta a_2 - \Delta a_3)$	$S_{21} = \sqrt{2}^{-1}(\Delta a_{11} - \Delta a_{12})$
$S_{11} = \sqrt{6}^{-1}(\Delta a_8 + \Delta a_9 + \Delta a_{10} - \Delta a_5 - \Delta a_6 - \Delta a_7)$	$S_{22} = \Delta a_{14}$

For the description of the internal coordinates, see Fig. 1.

TABLE II. Valence Force Constants^{a)} of Aspirin

Ring part ^{b)}							
In-plane	K_T	6.139	K_S	5.125	H_Ω	1.152	
	$H_\Phi(A)$	0.753	$H_\Phi(B)$	0.754	H_ϕ	0.457	
	F_T^m	-0.134	F_T^o	0.749	F_T^p	0.377	
	$F_{\Phi r8}$	0.541	F_{Tr8}	0.747	F_{Tr1}	0.546	
	$F_{\Omega r1}$	-0.180	F_ϕ^m	-0.015	$F_{T\Phi(A)}$	0.098	
	$F_{T\Phi(B)}$	0.190	$F_{T\phi}$	0.087	$F_{T\Omega}$	0.011	
	Out-of-plane	H_μ	0.416	$H_M(A)$	0.505	$H_M(B)$	0.541
		H_Z	0.278	$f_{MM}(A)$	0.083	$f_{MM}(B)$	-0.027
		f_Z^o	-0.035	$f_{\mu Z}^m$	0.031	$f_{\mu Z}^o$	-0.146
		f_μ^o	-0.065	f_μ^p	-0.039	f_μ^m	-0.001
$H_M(A)$		0.532	$H_M(B)$	0.660			
-OCOCH ₃ part							
K_{r1}	4.437	K_{r2}	6.345	K_{r3}		12.203	
K_{r4}	3.456	K_{Me}	4.846				
$f(1, 2)^c$	0.701	$f(1, 8)$	0.268	$f(2, 3)$		1.235	
$f(2, 4)$	0.379	$f(2, 8)$	0.827	$f(2, 9)$		-0.543	
$f(2, 10)$	0.995	$f(3, 4)$	0.530	$f(3, 9)$		-0.418	
$f(3, 10)$	0.315	$f(4, 5)$	0.457	$f(4, 9)$		0.268	
$f(4, 10)$	0.048	$f(4, 11)$	-0.165	$f(5, 11)$		0.083	
$f(9, 10)$	-0.055	$f(8, 8)$	0.747	$f(9, 9)$		0.826	
$f(10, 10)$	1.028	$f(11, 11)$	0.469	$f(11, 12)$		0.030	
$f(\tau_{C-O})^d$	0.153	$f(\tau_{O-C})$	0.182	$f(\tau_{Me})$		0.100	
$f(7, 14), f(6, 12)$		-0.101	$f(7, 15), f(6, 13)$			0.142	
$f(14, 14), f(12, 12)$		0.504	$f(14, 15), f(12, 13)$			-0.041	
$f(15, 15), f(13, 13)$		0.620					
-COOH part							
K_{r8}	5.301	K_{r9}	10.116	K_{r10}		6.583	
K_{r11}	4.991						
$f(16, 17)$	0.958	$f(16, 18)$	0.292	$f(16, 20)$		-0.077	
$f(16, 21)$	0.279	$f(17, 18)$	0.516	$f(20, 17)$		-0.077	
$f(21, 17)$	0.602	$f(18, 19)$	0.468	$f(20, 18)$		0.052	
$f(21, 18)$	-0.156	$f(22, 18)$	0.332	$f(22, 19)$		0.267	
$f(20, 20)$	0.462	$f(20, 21)$	0.007	$f(21, 21)$		1.555	
$f(22, 22)$	0.988	$f(\tau_{CC*})$	0.439	$f(\tau_{C*-O})$		0.367	
$f(\tau_{C*-O}, \gamma_{C*=O})^e$		1.118	$K_{\nu_{C*=O}}^{ab}$			-0.600 ^{f)}	

a) Stretching constants are in units of mdyn/Å; stretch-bend, mdyn/rad.; bending and torsion, mdyn Å/(rad.)². mdyn = 10⁻⁸ N. b) (A) is for the side of the -OCOCH₃ group, and (B) the -COOH group. c) See Table I for the numbers in parentheses; they indicate the symmetry coordinates. d) τ : torsion. e) γ : out-of-plane bending. f) Coupling force constant, see ref. 3.

coordinates for the two substituent groups are listed in Table I.

The intramolecular force constants were transferred from phenyl acetate⁴⁾ except for those around the carboxyl group, which were taken from benzoic acid.³⁾ The 89 general valence type force constants used in the last calculation are listed with one empirical coupling force constant in Table II.

Calculation of IR Intensities

We have adopted the effective atomic charge model which includes both the equilibrium charges and their first-order fluxes with respect to internal coordinates.⁸⁾

As in the case of phenyl acetate⁴⁾ and benzoic acid,³⁾ the charges of the phenyl group of aspirin calculated by the INDO method⁹⁾ are too small to reproduce the observed IR intensities. Consequently, those for the phenyl group were transferred from toluene,¹⁰⁾ while the charges calculated by the INDO method were used for the two substituents with a slight

TABLE III. Equilibrium Charges (e) and Charge Fluxes ($e\text{\AA}^{-1}$)

Equilibrium charges			
O1: -0.302 (-0.409) ^{a)}	O2: -0.415 (-0.303)	O3: -0.323 (-0.323)	
O4: -0.364 (-0.364)	H1: 0.331 (0.178)	C*: 0.336 (0.504)	
C': 0.516 (0.516)	C'': -0.081 (-0.081)	H6: 0.068 (0.002)	
H7: 0.068 (0.032)	H8: 0.068 (0.051)		
C1: 0.016	C2, C5: -0.127	C3, C4: -0.126	C6: 0.108
H2, H5: 0.114	H3, H4: 0.126		
Charge fluxes			
A - B - C	$\partial e_A / \partial R_i$	$\partial e_B / \partial R_i$	$\partial e_C / \partial R_i$
C1 - C6	-0.20	0.20	
C6 - C5	0.30	-0.30	
C6 - O3	0.25	-0.25	
C' - O4	0.45	-0.45	
C' - C''	0.42	-0.42	
H2 - C2 - C1	0.00	-0.20	0.20

^{a)} For the numbering of the atoms, see Fig. 1. The charges calculated by the INDO method are compared in parentheses.

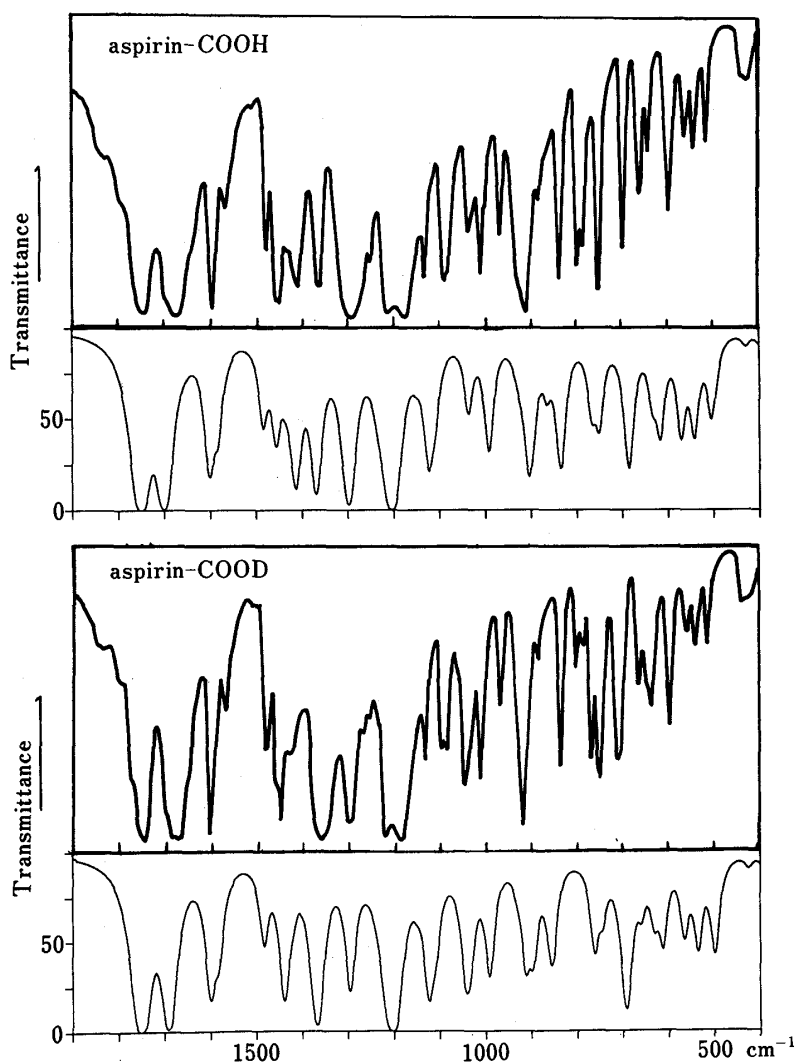


Fig. 2. Observed (Upper) and Simulated (Lower) IR Spectra of Aspirin and Aspirin-O-d

TABLE IV. Calculated $(\partial M/\partial Q_i)^2$ of Aspirin and Its -COOD Analogue in $(e/\sqrt{\text{amu}})^2$ ^{a)}

$\text{C}_6\text{H}_4(\text{OCOCH}_3)\text{COOH}$				$\text{C}_6\text{H}_4(\text{OCOCH}_3)\text{COOD}$			
$i^{b)}$		i		i		i	
9	0.3207	10	0.2178	9	0.3199	10	0.1786
11	0.0592	12	0.0273	11	0.0607	12	0.0275
13	0.0179	14	0.0328	13	0.0177	14	0.0559
15	0.0076	16	0.0071	15	0.0085	16	0.0067
17	0.0762	18	0.1024	17	0.0481	18	0.1011
19	0.1033	20	0.0432	19	0.0621	20	0.0103
21	0.0231	22	0.0074	21	0.0097	22	0.2364
23	0.2261	24	0.0039	23	0.0038	24	0.0598
25	0.0506	26	0.0123	25	0.0156	26	0.0440
27	0.0219	28	0.0022	27	0.0235	28	0.0128
29	0.0509	30	0.0002	29	0.0521	30	0.0003
31	0.0021	32	0.0143	31	0.0037	32	0.0501
33	0.0617	34	0.0063	33	0.0220	34	0.0032
35	0.0012	36	0.0663	35	0.0307	36	0.0321
37	0.0168	38	0.0404	37	0.0219	38	0.0802
39	0.0459	40	0.0348	39	0.0035	40	0.0355
41	0.0246	42	0.0373	41	0.0192	42	0.0255
43	0.0303	44	0.0271	43	0.0223	44	0.0381
45	0.0020	46	0.0044	45	0.0021	46	0.0040
47	0.0131	48	0.0096	47	0.0116	48	0.0098
49	0.0179	50	0.0041	49	0.0182	50	0.0044
51	0.0005	52	0.0031	51	0.0005	52	0.0028
53	0.0009			53	0.0012		

a) The integrated IR intensity of the i -th fundamental absorption band, A_i , can be calculated as follows: $A_i = 9.7488 \times 10^5 (\partial M/\partial Q_i)^2$ (m/mol), where M is the molecular dipole moment and Q_i the i -th normal coordinate.⁸⁾ b) Corresponds with the i in Table V.

adjustment, as done with phenyl acetate and benzoic acid. The equilibrium charges and the charge fluxes used in the last calculation are listed in Table III, where the values of equilibrium charges of the substituents calculated by the INDO method⁹⁾ are also given in parentheses.

The absorbances between 400 and 1900 cm^{-1} were calculated at intervals of 1 cm^{-1} by assuming the Lorentzian band shape with a common half-width of 20 cm^{-1} for all the fundamentals. This half-width was chosen so as to reproduce the peak absorbances measured at $cl = 7 \times 10^{-2}$ mol m^{-2} and the spectral band width of 1 cm^{-1} . The simulated IR spectra are compared with those observed in Fig. 2, and the calculated IR intensities are listed in Table IV.

Results and Discussion

The observed far-IR and Raman spectra of aspirin are shown in Figs. 3 and 4, respectively, and the observed frequencies are listed in Table V with the calculated values.

In the spectral region between 1800 and 1000 cm^{-1} , the simulated IR spectra reproduced the observed data fairly well, as shown in Fig. 2, but they did not do so in the lower frequency region. Since the frequency calculation was carried out by using the transferred force constants without any refinement and the number of intensity parameters (charges and charge fluxes) is less than half the number of normal modes, some disparity between the simulated and the observed spectra was inevitable.

In our previous work on benzoic acid,³⁾ we assigned the two IR bands at 804 and 810 to

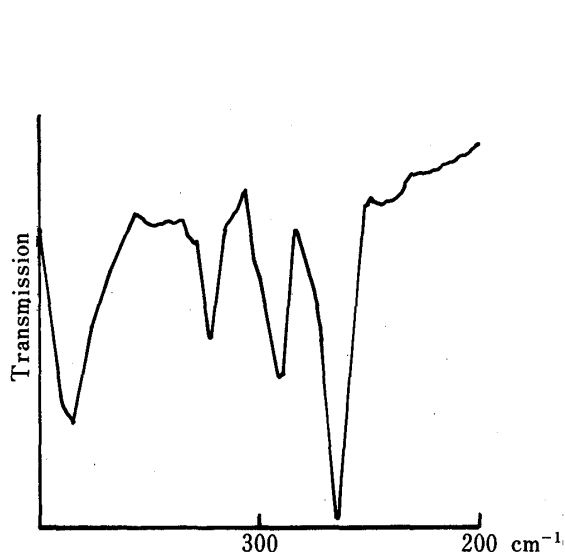


Fig. 3. Far-IR Spectrum of Aspirin (400—200 cm^{-1})

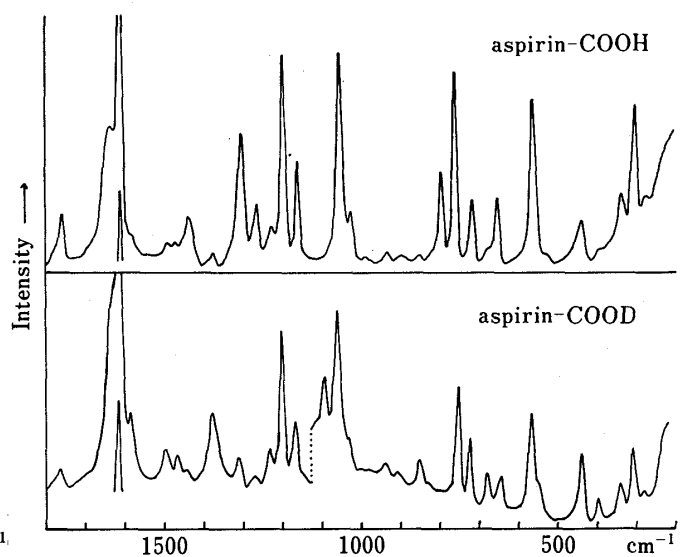


Fig. 4. Raman Spectra of Aspirin and Aspirin-O-d

the phenyl-carboxyl C-C stretching mode coupled with the ring breathing,¹¹⁾ and ν_{11} ¹²⁾ in Wilson's notation,¹³⁾ respectively. The latter is not affected by the deuteration of the carboxyl group, while the former is shifted about 20 cm^{-1} down. In the IR spectrum of aspirin, there are two similar bands at 802 and 788 cm^{-1} . Both these bands disappear on deuteration of the carboxylate group. According to the normal coordinate analysis, the band at 788 cm^{-1} was assigned to the C_1-C^* stretching vibration coupled with the breathing vibration, and that at 802 cm^{-1} to the C^*-O_2 torsion mode coupled with the $-C^*O_1$ out-of-plane bending mode. The C^*-O_2 torsion mode gives rise to a strong IR band at 918 cm^{-1} in analogy with the other carboxylic acids.¹⁴⁾

The crystal structure of aspirin is monoclinic $P2_1/c-C_{2h}^5$ with two cyclic dimers in a Bravais unit cell.¹⁾ As seen for many other simple carboxylic acids, large factor group splittings of the modes related to the $-COOH$ group are expected between the symmetric (g , Raman-active) and the antisymmetric (u , IR-active) species with respect to the center of symmetry between the two carboxyl groups.^{3,15)} The strong IR band at 1685 cm^{-1} and the Raman band at 1631 cm^{-1} are assigned to the $C^*=O_1$ stretching modes belonging to the u and g species, respectively, of site symmetry C_i of the ring dimer of the carboxylic acid. To reproduce this splitting in the calculation, we should introduce an empirical coupling force constant of -0.6 m dyn/\AA .^{3,15)}

The IR bands at 1460 and 1427 cm^{-1} are assigned to two complicatedly mixed vibrations in which the amplitudes of the O_2-H_1 in-plane deformation are large. Their Raman counterparts appear at higher frequencies, 1481 and 1430 cm^{-1} , respectively, as predicted by the calculation. The O_2-D in-plane deformation mode of aspirin-COOD is isolated from the neighboring skeletal stretching modes. Its dimeric out-of-phase vibration (u) gives rise to a rather strong IR band at 1048 cm^{-1} . The corresponding Raman band (g , in-phase) appears at 1078 cm^{-1} with medium intensity. The IR band at 1286 cm^{-1} arises from the $O-H$ in-plane deformation coupled with C^*-O_2 stretching mode, and the Raman band at 1293 cm^{-1} is assigned to the in-phase mode of the ring dimer. The calculated frequencies followed these splittings very well too.

For the IR band at 802 cm^{-1} , the calculated $g-u$ splitting is -20 cm^{-1} . In the beginning the Raman band at 782 cm^{-1} was considered to correspond only to the IR band at 788 cm^{-1} . The calculation suggests, however, that the Raman counterpart of the IR band at 802 cm^{-1} is

TABLE V. Observed and Calculated Intermolecular Frequencies (cm^{-1}) and Assignments^{a)}

Aspirin-COOH Obsd. (ν_i)		<i>i</i>	Calc.			Assignments
Raman	IR		<i>Z_e</i> ^{b)}	<i>a_g</i> ^{c)}	<i>a_u</i> ^{c)}	
1752 w	1752 s	9	1753	1753 (-1)	1755 (2)	C'O4 s
1631 m	1685 s	10	1701	1648 (0)	1704 (1)	C*O1 s
1603 s	1607 s	11	1601	1603 (-1)	1603 (0)	CC s
1575 w	1573 w	12	1583	1585 (0)	1585 (0)	CC s
	1485 m	13	1484	1509 (1)	1487 (1)	CC s+CH i b
1481 w	1460 m	14	1457	1486 (0)	1462 (-3)	O2H1 i d+CC s+C*O2 s
1457 w	1455 m					753+702
	1435 w	15	1436	1441 (0)	1441 (0)	Me i as d
	1422 w	16	1421	1424 (0)	1425 (3)	Me o as d
1430 w	1417 m	17	1414	1436 (0)	1424 (1)	O2H1 i d+C*O2 s+CH i b
1370 w	1372 m	18	1369	1371 (-2)	1372 (-1)	Me sym d
1301 m	1303 s	20	1296	1297 (0)	1297 (0)	CC s
1293 m	1286 s	19	1299	1331 (-1)	1315 (2)	O2H1 i d+C*O2 s+C*C s
	1265 w					970+291
1258 w	1255 w	21	1233	1238 (0)	1237 (0)	CH i b
1222 w	1219 s	22	1215	1219 (0)	1219 (-1)	ring i d+C6O3 s
1190 m	1190 s	23	1204	1205 (0)	1205 (0)	O3C' s+Me i r+C'O4 i r
1152 w		24	1150	1162 (-3)	1162 (-3)	CH i b
	1134 w					839+291
	1095 m	25	1123	1127 (-4)	1128 (-4)	CC s+CH i b
	1085 m	26	1110	1114 (0)	1114 (2)	CC s+C*O2 s
1042 m	1039 m	28	1034	1040 (2)	1040 (2)	CC s
	1031 sh	27	1037	1042 (0)	1041 (0)	Me o r
1012 w	1013 m	29	995	999 (0)	1000 (1)	Me i r+O3C' s
973 w	970 w	30	989	997 (-2)	997 (-1)	CH o d
		31	936	942 (-4)	958 (7)	CH o d
922 w	922 sh	32	926	934 (2)	934 (-8)	CH o d+C*O2 t
	918 s	33	909	912 (0)	915 (-2)	C'C'' s+O3C' s
883 w	885 w	34	896	903 (6)	905 (-2)	CH o d
835 w	839 s	35	868	871 (-1)	872 (0)	ring i d+C6O3 s
782 w	802 s	36	836	831 (-3)	853 (2)	C*O2 t+C*O1 o b
782 w	788 s	37	768	777 (1)	775 (-1)	CC s+C*C s
749 m	753 s	38	753	758 (0)	760 (6)	CH o d+ring t
705 w	702 s	39	686	693 (-1)	691 (-1)	ring t
666 w	663 m	40	637	639 (0)	639 (0)	C'O4 o b
640 w	642 w	41	623	626 (0)	627 (0)	ring i d+C''O'O3 i b
	596 m	42	572	578 (-1)	583 (-1)	ring i d+C*O1 i r
	563 w	43	544	551 (1)	550 (-3)	C'O i r
549 m	544 w	44	505	528 (0)	527 (0)	C''C'O3 i b+C'O4 i r
518 w	513 w	45	495	500 (-1)	500 (0)	ring t
	437 w	46	429	435 (-3)	438 (2)	ring t
427 w	427 w					266+162
380 w	383 m	47	384	393 (0)	397 (0)	C6O3 i r
325 w	322 w					162×2
291 m	291 w	48	316	326 (-2)	326 (1)	C''C'O3 i b
		49	264	296 (1)	281 (2)	C1C*O2 i b
261 w	266 m	50	254	273 (2)	274 (6)	ring t+C1C* o b
		51	249	264 (2)	260 (-3)	Me t
162 s		52	180	215 (5)	204 (0)	C*C i r
		53	168	191 (1)	187 (-1)	C1C* t
		54	82	90 (0)		C6O3 o b
		55	74	84 (-4)		O3C' t
77 ^{d)}		56	53	70 (-6)		C6O3 t

TABLE V. (continued)

Aspirin-COOD		<i>i</i>	Calc. ^{b)}	Assignments
Obsd. (ν_i)				
Raman	IR			
1752 w	1752 s	9	1753	C'O4 s
1628 sh	1685 s	10	1692	C*O1 s
1603 s	1607 s	11	1600	CC s
1575 w	1573 w	12	1583	CC s
1478 w	1482 m	13	1484	CC s+CH i b
1455 w	1453 m	14	1440	CC s+CH i b, 753+702
	1435 w	15	1436	Me i as d
	1422 w	16	1421	Me o as d
1371 m	1372 s	17	1370	Me sym d
		18	1369	C*O2 s+C*C1 s
1301 w	1303 m	19	1296	CC s
1259 w	1255 w	20	1234	CH i b
1224 w	1215 s	21	1215	ring i d+C6O3 s
1190 m	1185 s	22	1205	O3C' s+Me i r+C'O4 i r
1152 w		23	1150	CH i b
	1132 w			839+291
	1095 m	24	1124	CC s+CH i b
	1085 m	25	1110	CC s+C*O2 s
1078 m	1048 m	26	1044	O2H1 i d
1042 m	1039 sh	27	1037	Me o r
		28	1033	CC s
1014 sh	1013 m	29	995	Me i r+O3C' s
	970 w	30	989	CH o d
		31	933	CH o d
923 w	918 s	32	913	O3C' s+C'C'' s
886 w	885 w	33	899	CH o d
835 w	835 m	34	865	ring i d+C6O3 s
		35	857	ring t+C*O1 o b
	770 m	37	748	CC s+C1C* s
742 m	749 m	36	764	CH o d
708 m	710 m	38	693	ring t+C*O2 t+C6O3 o b
662 w	661 w	39	660	C*O2 t+C'C'' o b
	642 sh	40	632	C'C'' o b+ring t
603 w	635 w	41	614	ring t
	596 m	42	567	ring i d+C*O1 i r
	563 w	43	537	C'O4 i r+C'C'' s+ring i d
549 m	544 w	44	501	C'O4 i r+C''C'O3 i b
	513 w	45	495	ring t
	437 w	46	426	ring t
427 w	427 w			266+162
380 w		47	380	C6O3 i r
325 w				162×2
291 w		48	314	C''C'O3 i b
		49	261	C1C*O2 i b
261 w		50	250	ring t+C1C* o b
		51	249	Me t
162 s		52	175	C6O3 i r
		53	147	ring t

a) Schematic description verified by calculation; the meanings of symbols are as follows: i (in-plane), o (out-of-plane), s (stretching), b (bending), r (rocking), d (deformation), t (torsion), sym (symmetric), as (asymmetric). b) Calculated frequencies of the isolated molecular model. c) The a_g and a_u frequencies are shown together with the splittings in parentheses: $\nu(a_g) - \nu(b_g)$ for Raman and $\nu(a_u) - \nu(b_u)$ for IR. d) It was observed in the b_g Raman spectrum, see Fig. 6.

TABLE VI. Observed and Calculated Lattice Vibrations (cm^{-1}) of Aspirin Single Crystal

a_g		b_g	
Calc.	Obsd.	Calc.	Obsd.
121	123	124	128
102	113	114	112
96	94	95	95
66	66 (63)	61	61
46	46	43	46
42	40	37	40

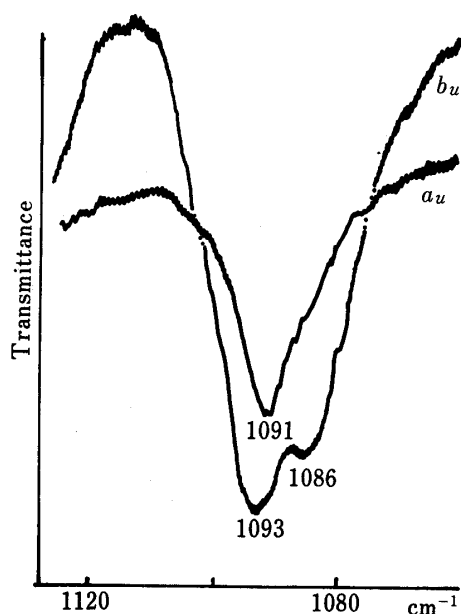


Fig. 5. Polarized IR Spectra of Aspirin Single Crystal ($1120\text{--}1060\text{ cm}^{-1}$)

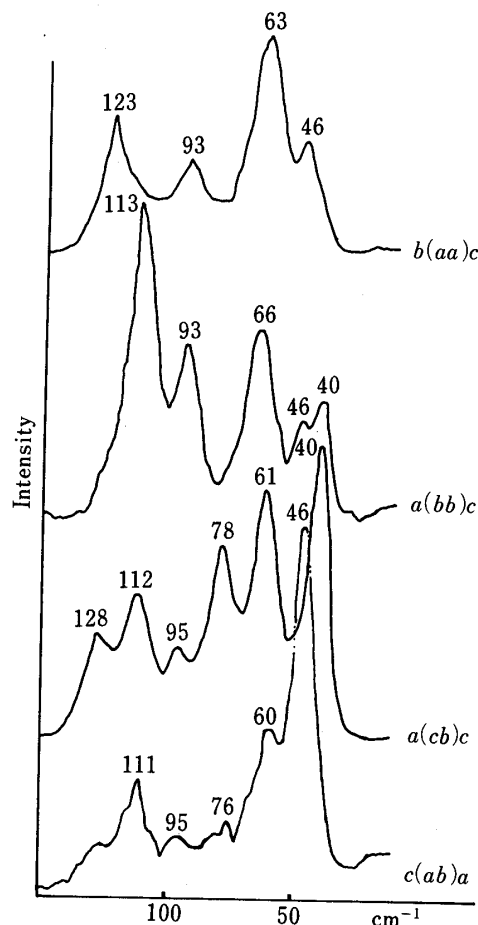


Fig. 6. Polarized Raman Spectra of Aspirin Single Crystal between $150\text{ and }20\text{ cm}^{-1}$

also overlapping on it.

In the region between $1080\text{ and }1100\text{ cm}^{-1}$ where two normal frequencies (ν_{25} and ν_{26} in Table V) are expected, only one IR band appears in the a_u IR spectrum, while two bands appear in the b_u spectrum, as shown in Fig. 5. In accord with the observed spectra, the calculated separation between ν_{25} and ν_{26} in the b_u species is larger than that in the a_u species.

The polarized Raman spectra below 150 cm^{-1} of aspirin crystal are shown in Fig. 6. As listed in Table V, the band at $78(6)\text{ cm}^{-1}$ of the b_g spectra was assigned to an intramolecular vibrational mode by calculation. The observed lattice frequencies are compared with the calculated values in Table VI. They agree with each other very well.

As a whole, the potential parameters adopted in this work were consistent with the vibrational spectra of aspirin crystal, and by simulation of the IR spectra, we could obtain an empirical set of atomic charges and their fluxes. Employing these charges, we recalculated the specific surface energies of the various crystalline faces *in vacuo* ($D=1.0$) according to the method described previously.²⁾ The results are listed in Table VII along with the contribution of V_2 to the surface energy of each crystal plane. In comparison with the values calculated with the INDO charges,²⁾ the specific surface energies of the three crystalline faces (011), (110)

TABLE VII. Specific Surface Energy (E_{hkl})^{a)} of Aspirin Crystal Calculated with the Empirical Charges Obtained from the Infrared Intensities

Surf.	$(hkl)^b$	$E_{hkl} = V_1 + V_2 + V_3$		V_2^c
		$D = 1.0$	$D = 78.56$	
<i>ab</i>	(004)	176.4	157.7	0.0
<i>bc</i>	(200)	141.5	127.3	0.0
<i>ca</i>	(011)	394.9	275.8	92.0
<i>ca</i>	(110)	316.6	254.7	46.0
<i>ca</i>	(020)	658.1	458.0	160.0

a) In units of mJm^{-2} . b) The symbol (hkl) is employed here instead of $(hkl)/P$ used previously.²⁾ c) In Table IV of the previous work,²⁾ we erroneously listed $V_1 + V_3$ instead of $V_1 + V_2 + V_3$. The correct values of $V_1 + V_2 + V_3$ for the INDO charges are obtained by adding these V_2 energies to them. The Coulombic part of the hydrogen bond energy is included in V_3 according to the definition of the Lippincott function.⁶⁾

and (010) forming the face *ca* were increased by 23% on average, while the surface energies of the face *ab* (001) and the face *bc* (100) were almost unchanged. The increase of the calculated surface energy of face *ca* might be attributed to the large value of the sum of the changes in the atomic charges of the phenyl group, which is closest to face *ca*.

As in our previous work,²⁾ the surface energy of each crystal plane was calculated by using the dielectric constant of water (78.56). As in the case of the INDO charges, the surface energies of (011), (110) and (010) are much more sensitive to the dielectric constant in V_3 than are those of (001) and (100). The decrease of surface energy on changing the dielectric constant in V_3 from 1 to 78.56 may be taken to represent the stabilization energy of the surface on transferring the crystal from a nonpolar solvent to water. The interpretation of the least area-diminishing velocity of face *ca*²⁾ as being due to this stabilization energy is not altered by changing the source of the atomic charges from the INDO calculation to the infrared band intensities.

Acknowledgement The numerical calculations were carried out on a FACOM M382 computer at the Data Processing Center of Kyoto University.

References

- 1) Y. Kim, K. Machida, T. Taga and K. Osaki, *Chem. Pharm. Bull.*, **33**, 2641 (1985).
- 2) Y. Kim, M. Matsumoto and K. Machida, *Chem. Pharm. Bull.*, **33**, 4125 (1985).
- 3) Y. Kim and K. Machida, *Spectrochim. Acta*, **42A**, to be published (1986).
- 4) Y. Kim, H. Noma and K. Machida, *Spectrochim. Acta*, **42A**, to be published (1986).
- 5) I. Harada and T. Shimanouchi, *J. Chem. Phys.*, **44**, 2016 (1966).
- 6) a) E. R. Lippincott, *J. Chem. Phys.*, **21**, 2070 (1953); b) E. R. Lippincott and R. Schroeder, *ibid.*, **23**, 1099 (1955).
- 7) D. E. Williams, *Acta Crystallogr., Sect. A*, **27**, 452 (1971).
- 8) A. J. van Straten and W. M. A. Smit, *J. Chem. Phys.*, **67**, 970 (1977).
- 9) J. A. Pople and D. L. Beveridge, "Approximate Molecular Orbital Theory," McGraw-Hill, New York, 1970.
- 10) M. Akiyama, *Spectrochim. Acta*, **40A**, 781 (1984).
- 11) G. Varsanyi, "Vibrational Spectra of Benzene Derivatives," Academic Press, New York and London, 1969, pp. 219–221.
- 12) G. Varsanyi, "Vibrational Spectra of Benzene Derivatives," Academic Press, New York and London, 1969, pp. 336–337.
- 13) E. B. Wilson, *JR, Phys. Rev.*, **45**, 706 (1934).
- 14) S. Hayashi and J. Umemura, *J. Chem. Phys.*, **63**, 1732 (1975).
- 15) J. Umemura, *J. Mol. Struct.*, **36**, 35 (1977).